ACCOUNTS
of chemical research

Two-Dimensional Infrared Spectroscopy of Intermolecular Hydrogen Bonds in the Condensed Phase

THOMAS ELSAESSER
Max-Born-Institut für Nichtlineare Optik und Kurzzeitspektroskopie, D-12489 Berlin, Germany

RECEIVED ON JANUARY 6, 2009

CONSPECTUS

Hydrogen bonding plays a key role in the structural, physical, and chemical properties of liquids such as water and in macromolecular structures such as proteins. Vibrational spectroscopy is an important tool for understanding hydrogen bonding because it provides a way to observe local molecular geometries and their interaction with the environment. Linear vibrational spectroscopy has mapped characteristic changes of vibrational spectra and the occurrence of new bands that form upon hydrogen bonding. However, linear vibrational spectroscopy gives very limited insight into ultrafast dynamics of the underlying molecular interactions, such as the motions of hydrogen-bonded groups, energy dissipation and delocalization, and the fluctuations within hydrogen-bonded structures that occur in the ultrafast time domain. Nonlinear vibrational spectroscopy with its femtosecond time resolution can discern these dynamic processes in real time and has emerged as an important tool for unraveling molecular dynamics and for quantifying interactions that govern the vibrational and structural dynamics of hydrogen bonds. This Account reviews recent progress originating from third-order nonlinear methods of coherent multidimensional vibrational spectroscopy.

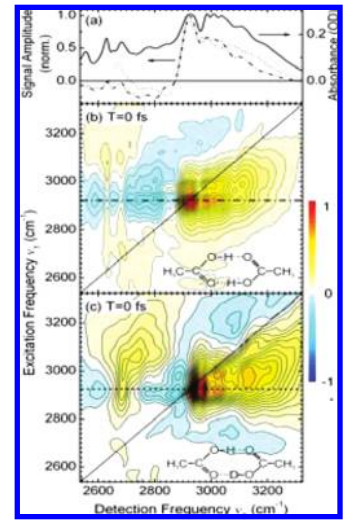

Ultrafast dynamics of intermolecular hydrogen bonds are addressed for a number of prototype systems: hydrogen-bonded carboxylic acid dimers in an aprotic liquid environment, the disordered fluctuating hydrogen-bond network of liquid water, and DNA oligomers interacting with water. Cyclic carboxylic acid dimers display a rich scheme of vibrational couplings, resulting in OH stretching absorption bands with highly complex spectral envelopes. Two-dimensional spectroscopy of acetic acid dimers in a nonpolar liquid environment demonstrates that multiple Fermi resonances of the OH stretching mode with overtones and combination tones of fingerprint vibrations dominate both the 2D and linear absorption spectra. The coupling of the OH stretching mode with low-frequency hydrogen-bonding modes leads to additional progressions and coherent low-frequency hydrogen-bond motions in the subpicosecond time domain. In water, the 2D spectra reveal ultrafast spectral diffusion on a sub-100 fs time scale caused by the ultrafast structural fluctuations of the strongly coupled hydrogen-bond network. Librational motions play a key role for the ultrafast loss of structural memory. Spectral diffusion rates are enhanced by resonant transfer of OH stretching quanta between water molecules, typically occurring on a 100 fs time scale. In DNA oligomers, femtosecond nonlinear vibrational spectroscopy resolves NH and OH stretching bands in the highly congested infrared spectra of these molecules, which contain alternating adenine−thymine pairs. Studies at different levels of hydration reveal the spectral signatures of water molecules directly interacting with the phosphate groups of DNA and of a second water species forming a fluctuating environment around the DNA oligomers. We expect that the application of 2D infrared spectroscopy in an extended spectral range will reveal the intrinsic coupling between water and specific functional units of DNA.

1. Introduction

Hydrogen bonding represents a fundamental local interaction in nature.[1] A hydrogen bond X−H···Y is mediated through the attractive interaction between a hydrogen donor group X−H (X = O, N, F) and a neighboring electronegative acceptor atom Y (Y = O, N, F, Cl), resulting in a binding energy of 4−40 kJ/mol, a fraction of that of covalent bonds. The attractive Coulomb interaction

Published on the Web 05/08/2009 www.pubs.acs.org/acr
10.1021/ar900006u CCC: $71.50

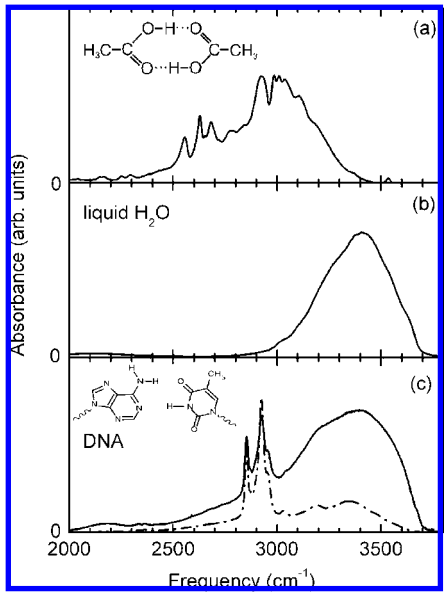

FIGURE 1. Vibrational OH stretching absorption bands of (a) cyclic dimers of acetic acid dissolved in CCl_4 (inset, dimer structure, concentration 0.8 M) and (b) liquid water and (c) vibrational spectra of an isotropic thin-film sample of DNA oligomers containing 23 alternating adenine−thymine base pairs at a hydration level of 0% relative humidity (RH, dash-dotted line) and 92% RH (solid line). N−H stretching modes of the bases and the O−H stretching mode of water contribute to the broad absorption above 3000 cm^{-1}. The absorption peaks between 2800 and 3000 cm^{-1} are due to CH stretching modes.

between the hydrogen and the acceptor atom, van der Waals and dispersion forces, and, in strong hydrogen bonds, covalent contributions are the main interaction mechanisms.[2] The binding energy is high enough to define molecular structure such as hydrogen-bonded dimers and biological macromolecules. The limited bond strength, on the other hand, allows for structural changes and fluctuations by "making and breaking" hydrogen bonds.

Vibrational spectroscopy is a major tool of hydrogen-bond research because it can grasp local molecular geometries and their interaction with the environment. Steady-state linear infrared and Raman spectroscopy have been applied extensively to map the occurrence of new vibrational bands and characteristic changes of frequency position and line shape of existing bands upon hydrogen-bond formation.[2] Such work has mainly addressed the vibrations of the hydrogen donor groups as illustrated in Figure 1 for the OH stretching absorption of (a) cyclic dimers of acetic acid in a nonpolar environment, (b) liquid H_2O, and (c) the congested NH and OH stretching absorption of hydrated films of DNA oligomers. Compared with free OH and NH groups, the spectra display a shift to lower frequencies, which indicates the reduction of the vibrational force constant by hydrogen bonding, and a strongly enhanced absorption with broad and highly complex spectral line shapes. In general, time-dependent structural disorder leading to a distribution of hydrogen-bond strengths and vibrational couplings to other modes or a fluctuating environment cause such spectral envelopes. In condensed phases, the underlying molecular dynamics occur in the ultrafast time domain between 10 fs and a few picoseconds. While linear vibrational spectroscopy does not allow for a decisive analysis of the molecular behavior, nonlinear vibrational spectroscopy with a femtosecond time resolution can discern different processes in real time.[3,4] Moreover, coherent two-dimensional (2D) vibrational spectroscopy provides direct quantitative insight into vibrational couplings and their role for vibrational dynamics.[5−9]

In this Account, the potential of 2D vibrational spectroscopy is illustrated by discussing three prototypes of hydrogen-bonded systems. Cyclic acetic acid dimers with two intermolecular hydrogen bonds display a well-defined time-independent planar structure, that is, negligible structural disorder or fluctuations. Femtosecond infrared pump−probe and 2D spectroscopy reveal couplings between vibrational modes including low-frequency hydrogen-bond modes in great detail (section 3). Liquid H_2O, an extended network of highly polar hydrogen-bonded molecules, exhibits pronounced structural disorder and fluctuations on a multitude of time scales. The ultrafast loss of structural correlations in this system leads, together with resonant energy transfer between the molecules, to ultrafast spectral diffusion that is mapped directly by 2D spectroscopy (section 4). DNA in an aqueous environment combines both types of behavior. The double helix and, in particular, the base pairs of DNA represent well-defined hydrogen-bonded structures, which interact with water molecules in their environment. Both specific local interactions of water with, for example, NH or CO groups of bases or phosphate groups in the DNA backbone, and fluctuating long-range Coulomb interactions play a role in the dynamics of this biomolecular model system.

2. Ultrafast Coherent Infrared Spectroscopy of Hydrogen Bonds

Femtosecond infrared spectroscopy is based on the resonant interaction of femtosecond light pulses with vibrational dipole transitions and, in most cases, maps the third-order nonlinear response of the molecular ensemble. Infrared pulses of $\leq$100 fs duration are available in a wide wavelength range from 2.5 to 20 μm (frequency range 4000−500 cm^{-1}), covering a major part of the vibrational spectrum of hydrogen

bonds.[10,11] While a direct infrared excitation below 500 cm^{-1} has not been accomplished, anharmonic coupling of such modes to high-frequency vibrations allows for studying their transient behavior as well.[12]

Femtosecond resonant excitation of a transition between two quantum states of an oscillator generates both a coherent polarization, that is, a dipole-mediated superposition of the quantum-mechanical wave functions of the two states, and a population change by promoting molecules from the lower to the upper state. The time evolution of transient polarizations and populations is governed by microscopic molecular couplings giving rise to spectral diffusion or vibrational dephasing, population and orientational relaxation, and energy redistribution and transfer. A variety of pump−probe and photon-echo techniques allow for measuring transient polarizations and populations by mapping the nonlinear third-order response as a function of time and frequency.[3,4] In 2D infrared spectroscopy, the third-order response function of the molecular ensemble is read out by determining the third-order polarization as a function of two frequencies, the excitation frequency ν_1 and the detection frequency ν_3.[5−9] There are different experimental implementations of 2D infrared spectroscopy, in particular the double-resonance or dynamic hole burning method,[5,13] a special type of two-color pump−probe spectroscopy,[14,15] and Fourier transform spectroscopy based on heterodyne-detected three-pulse photon echoes.[6−9,16] From the photon echo signal, one derives 2D spectra by Fourier-transforming the time-dependent third-order polarization. The real part of this quantity gives the absorptive and the imaginary part the dispersive response of the sample.

In Figure 2, two limiting cases of 2D infrared spectra of hydrogen-bonded systems are illustrated schematically. In case of coupled vibrational transitions at fixed frequency positions, that is, negligible spectral diffusion, the complex envelope of the linear infrared spectrum is made up of a series of partly overlapping absorption peaks (left panel of Figure 2a). In the absorptive 2D spectrum, couplings between the different components show up directly (right panel): Whenever a particular transition is excited (blue or red profile), it gives rise to an absorptive signal at the same frequency, that is, on the diagonal of the 2D spectrum (blue and red symbols), and to off-diagonal peaks at the frequency position of the other coupled transition (black symbols). In this way, complex coupling schemes are deciphered with the strength of the off-diagonal peaks reflecting the strength of the couplings. Cyclic acetic acid dimers represent a prototype of such behavior (see section 3). The schematic 2D spectrum in Figure 2a neglects the substructure of the individual peaks, in general consisting of

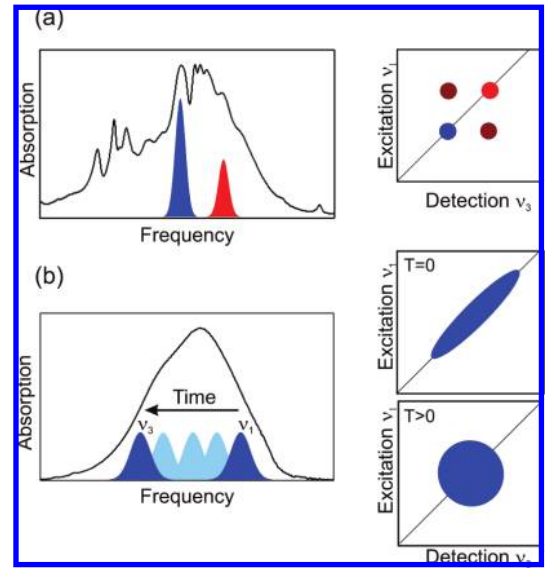

FIGURE 2. (a) Schematic of coupled transitions in the linear OH stretching absorption (solid line) of acetic acid dimers. The couplings give rise to off-diagonal peaks in the nonlinear 2D spectrum (black circles, right panel). (b) Schematic of spectral diffusion in water. Left panel: Inhomogeneously broadened OH stretching absorption band of water (black solid line). Structural fluctuations lead to spectral diffusion, an ultrafast shift of the transition frequency from its initial value ν_1 to ν_3. Right panel: In the 2D spectra, spectral diffusion destroys the initial correlation of excitation and detection frequencies within T (population time).

an absorption decrease on the $\nu = 0$ to 1 transition and an anharmonically red-shifted absorption increase on the $\nu = 1$ to 2 transition of the oscillator.

In Figure 2b, the case of spectral diffusion is illustrated. In a disordered hydrogen-bond network like water, the $\nu_{OH} = 0$ to 1 transition frequency of the OH stretching mode depends on the local environment, resulting in a (inhomogeneous) frequency distribution within the OH stretching band (left panel). As the structure of hydrogen-bond network and, thus, the local molecular environments fluctuate, the transition frequency of a particular oscillator undergoes stochastic shifts within the spectral envelope. In the linear infrared spectrum, this spectral diffusion shows up as a broadening giving no information on the underlying time scale. In contrast, 2D spectra (right panel) reveal such phenomena: 2D spectra for a "read-out" time $T = 0$ (population time $T = 0$, the second and third pulse in a three-pulse photon echo experiment interact simultaneously with the sample) reflect the initial distribution of transition frequencies, each excitation frequency ν_1 being correlated with the corresponding detection frequency ν_3 on the diagonal, $\nu_1 = \nu_3$. Spectral diffusion during a finite time interval T before the "read-out" destroys the correlation of ν_1 and ν_3, and the 2D spectrum for $T > 0$ shows an essentially round shape. The transition frequencies are now randomized

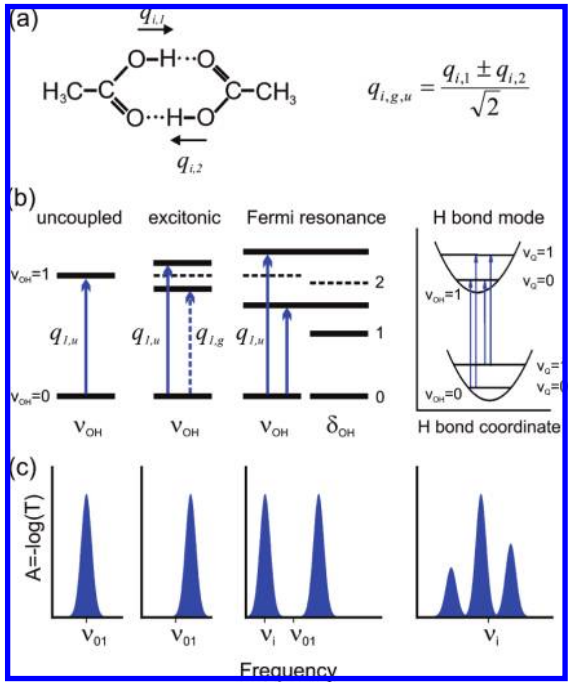

FIGURE 3. (a) Structure of cyclic acetic acid dimer and definition of symmetric vibrational coordinates $q_{i,g,u}$ ($q_{i,1}$, $q_{i,2}$ = local vibrational coordinates). (b) Schematic level schemes of the $\nu = 0$ to 1 OH stretching transition for different vibrational couplings: uncoupled dipole allowed transition (solid blue arrow, $q_{i,u}$ coordinate), splitting of the $\nu_{OH} = 1$ state due to excitonic coupling and infrared active transition in the $q_{i,u}$ coordinate (dashed arrow = Raman active transition in the $q_{i,g}$ coordinate), transitions for a Fermi resonance of the OH stretching and bending modes (dashed lines = uncoupled $\nu = 1/\nu = 2$ states of the OH stretching/bending mode), and potential energy diagram illustrating the anharmonic coupling of the OH stretching and a hydrogen-bond mode. (c) Schematic infrared absorption lines for the uncoupled oscillator and the three coupling cases. Excitonic coupling leads to an up-shifted single line, whereas Fermi resonances give rise to a pair of lines. On each line, side bands due to coupling of the hydrogen-bond mode occur.

and the system has lost its frequency and underlying structural "memory". Such behavior is discussed for neat H_2O in section 4.

3. Vibrational Couplings in Cyclic Acetic Acid Dimers

Cyclic dimers of acetic acid (Figures 1 and 3a) contain two intermolecular O−H···O hydrogen bonds in a planar geometry (C_{2h} symmetry). For a convenient description of their vibrational properties, symmetry coordinates $q_{i,g,u} = (q_{i,1} \pm q_{i,2})/\sqrt{2}$ have been introduced, which are linear combinations of the local vibrational coordinates $q_{i,1}$ and $q_{i,2}$ of the modes i (Figure 3a).[17] The symmetry coordinates show a gerade (g) and ungerade (u) symmetry with respect to the dimer's center of inversion and a symmetric or antisymmetric behavior with respect to the C_2 rotation axis perpendicular to the dimer plane.

In Figure 3b, the influence of different vibrational couplings on the OH stretching absorption is illustrated schematically.[4,17−19] In the absence of any anharmonic coupling, the infrared active OH stretching fundamental is due to the dipole-allowed transition between the $\nu = 0$ and 1 states in the $q_{1,u}$ coordinate (1 = OH stretching). The Raman active $\nu = 0$ to 1 transition in the $q_{1,g}$ coordinate occurs at the same frequency. Introducing an excitonic coupling V_0 between the two local OH stretching oscillators (coordinates $q_{1,1}$, $q_{1,2}$) results in a splitting of the $\nu = 1$ states in the $q_{1,u}$ and $q_{1,g}$ coordinates by $2V_0$ and a spectral shift of the infrared (Figure 3c) and the Raman active transition of opposite sign. A Fermi resonance of the $\nu = 1$ state of the $q_{1,u}$ mode with overtones and combination tones of fingerprint modes leads to a splitting of the $\nu = 1$ state and the occurrence of two dipole-allowed transitions (Figure 3b,c). In general, multiple Fermi resonances break the single OH stretching transition into a multitude of absorption lines. Finally, there exists a coupling between the OH stretching mode and hydrogen-bond modes of much lower frequency involving motions of the oxygen atoms and thus changing the hydrogen-bond geometry. In an adiabatic treatment of this coupling, the high-frequency OH stretching mode defines a potential for the quantized low-frequency hydrogen-bond mode (Figure 3b). The anharmonic coupling is manifested in an origin shift of the potentials for different states ν_{OH} of the high-frequency mode, giving rise to low-frequency progressions in the OH stretching absorption (Figure 3c). Low-frequency progressions exist on each of the fundamentals generated via the Fermi resonances.

In general, all couplings occur simultaneously and the OH stretching band displays many subcomponents. In liquids, the coupled system is subject to fluctuating forces exerted by the environment that induce vibrational dephasing.[20,21] While theoretical efforts analyzing the linear vibrational spectra have remained inconclusive with respect to the overall line shape, femtosecond pump−probe and 2D infrared spectroscopy combined with theoretical work have led to a quantitative understanding of the coupling schemes and the linear and nonlinear spectra of cyclic acetic acid dimers.[12,22−26] Three-pulse photon-echo experiments have demonstrated multilevel coherences of OH-stretching excitations, which are caused by the anharmonic coupling between the OH stretching and low-frequency hydrogen-bond modes.[23] The nonexponential decay of the macroscopic polarization reveals a 200 fs OH stretch dephasing time and multilevel quantum beats due to coher-

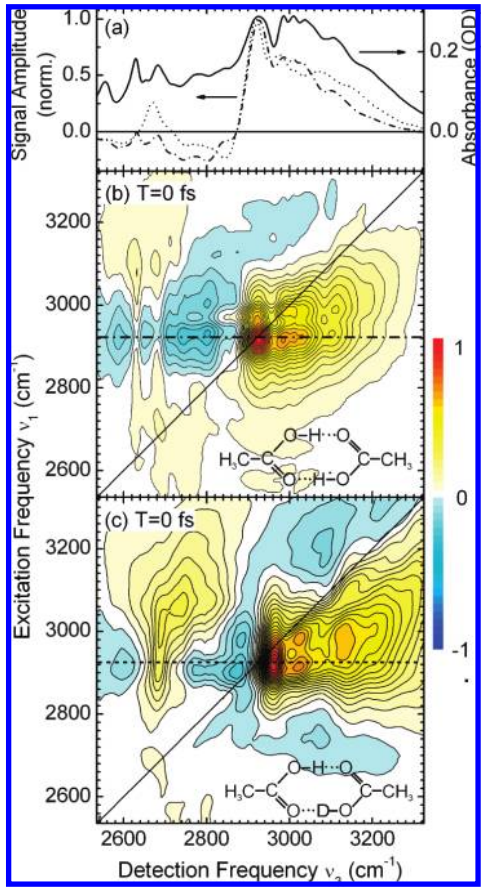

FIGURE 4. (a) OH stretching absorption band (solid line) and cross section of the 2D spectra at an excitation frequency of 2920 cm^{-1} of cyclic acetic acid OH/OH (dash-dotted line, panel b) and OH/OD (dotted line, panel c) dimers in CCl_4. (b) 2D spectrum of cyclic acetic acid dimers measured at a population time of $T = 0$ fs. The real part of the signal is plotted as a function of excitation and detection frequency. (c) 2D spectrum at $T = 0$ fs for the mixed dimer. Contour line spacings in the 2D spectra are equal to 0.049.

ent wavepacket motions along low-frequency hydrogen-bond modes. The low-frequency coherences decay on a picosecond time scale. Strong couplings exist between the OH stretching and the hydrogen-bond stretching mode at 170 cm^{-1} and the in-plane bending mode at 145 cm^{-1} with cubic coupling constants $|\Phi(i^2j)| \approx 150$ cm^{-1} (i = OH stretch, j = low-frequency mode).[12,22]

Two-dimensional infrared spectra give specific insight into the spectral substructure of the OH stretching absorption band.[24] In Figure 4b,c, 2D spectra measured for a population time $T = 0$ fs are shown for the OH/OH and OH/OD dimers, the latter containing one OH and one OD group. The absorptive 2D signal is plotted as a function of excitation and detection frequency with positive amplitudes in the range of the $\nu = 0$ to 1 transitions and negative amplitudes on the partly overlapping $\nu = 1$ to 2 transitions that are anharmonically red-shifted. The latter contribution is absent in 2D spectra at $T = 400$ fs (not shown) due to the 200 fs decay of the $\nu = 1$ state.[22,23] In the central part of the spectra, strong diagonal peaks occur at 2920 and 2990 cm^{-1}, together with their (off-diagonal) cross peaks. In addition, there are off-diagonal peaks at a variety of detection frequencies, as is evident from cross sections through the spectra for constant excitation frequency (Figure 4a). The cross section for the OH/OH dimers displays peak positions similar to the linear OH stretching absorption. The similar peak patterns for the OH/OH and OH/OD dimers point to a minor role of excitonic OH/OH coupling. The positions of both diagonal and off-diagonal peaks remain constant for longer population times T,[24] demonstrating a negligible spectral diffusion.

For an in-depth analysis, density functional theory calculations of vibrational eigenstates, couplings, and the linear vibrational spectrum were combined with a calculation of the 2D photon echo signals based on a sum-over-states formalism.[22,25−27] The calculations account for the linear absorption band and the 2D spectra in a quantitative way. The prominent off-diagonal peaks in the 2D spectra (Figure 4b,c) are due to the multiple Fermi resonance coupling mechanism. The multitude of resonances causes the multitude of off-diagonal peaks in the 2D spectra and the break-up of the linear spectrum into a multitude of lines. In addition to Fermi resonances, low-frequency mode progressions give rise to off-diagonal peaks, mostly, however, of minor intensities. The prominent peaks are due to Fermi resonances of the $\nu = 1$ state of the OH stretching mode with combination and overtones of fingerprint modes. The predominant third-order coupling to the (ungerade) OH stretching mode requires a combination of a Raman and an infrared-active fingerprint transition due to the symmetry of the vibrational wave functions. Combination tones occurring in the relevant frequency range involve the carbonyl (C═O) stretching, the OH bending, the CH_3 wagging, and the C−O stretching modes. These fingerprint modes contain considerable contributions of local OH bending motions, resulting in a strong coupling to the OH stretching mode. For the most prominent peaks, the cubic couplings have absolute values between 50 and 150 cm^{-1}, that is, are in the same range as the couplings to hydrogen-bond modes. This finding shows that all couplings need to be included to account for the linear and nonlinear infrared spectra.

4. Ultrafast Vibrational and Structural Dynamics of Water

The ultrafast structural fluctuations of the hydrogen-bond network in water are connected with multiple molecular rearrangements and the breaking and reformation of hydrogen bonds. The highly polar nature of water results in long-range

fluctuating Coulomb forces exerted on the anharmonic OH stretching oscillators in the network. This interaction leads to a femtosecond stochastic modulation, that is, spectral diffusion, of the fundamental transition frequency $\nu(0-1)$ over a range of 500 cm^{-1}.[28] The frequency modulation results in dephasing, the loss of quantum coherence of the optically coupled states of the anharmonic oscillator.[21] In neat H_2O, the transfer of OH stretching excitations via dipole coupling of neighboring water molecules[29] with slightly detuned $\nu(0-1)$ also contributes to spectral diffusion.

Spectral diffusion and vibrational dephasing were first investigated with HOD in D_2O or H_2O where the OH or OD stretching oscillators are highly diluted and resonant energy transfer is practically absent.[15,28−37] The first femtosecond two- and three-pulse photon-echo experiments have shown an initial 35 fs decay of the homodyne detected signal, followed by subpicosecond and picosecond kinetic components.[31,32] The hydrogen-bonded OH stretching oscillator displays a large diagonal anharmonicity $\Delta = \nu(0-1) - \nu(1-2) \approx 270$ cm^{-1}. Applying the approach of ref 21, one estimates a pure dephasing time of ~100 fs of the macroscopic OH stretching polarization, in qualitative agreement with the experiment. Detailed frequency fluctuation correlation functions have been derived from 2D spectra for both OH and OD stretching excitations of HOD. The correlation functions show sub-50-fs, 400-fs, and 1.4-ps decay components.[35,38] Different assignments were made for the microscopic mechanisms behind the correlation decay. The 400-fs component is in the range of the fastest orientational relaxation of HOD molecules ($\tau_{or} \approx 700$ fs[29]), whereas the picosecond component was assigned to hydrogen-bond breaking and making dynamics.

In the following, the behavior of H_2O is discussed.[16,39] In Figure 5, 2D spectra of the OH stretching mode are shown for different population times, that is, time delays T between the second and the third pulse interacting with the sample, a 400 nm thick film of H_2O. Such measurements were performed for a wide range of sample temperatures between 274 and 304 K. The yellow-red signal is due to the $\nu_{OH} = 0$ to 1 transition of the OH stretching oscillator, whereas the blue feature originates from the red-shifted $\nu = 1$ to 2 transition ($\Delta \approx 270$ cm^{-1}). For $T = 0$ fs, the $\nu_{OH} = 0$ to 1 spectra are stretched along the diagonal $\nu_1 = \nu_3$ (straight solid line), reflecting the initial inhomogeneous broadening due to distribution of molecular sites in the hydrogen-bond network. Such initial correlation of frequencies is lost on an ultrafast time scale. At room temperature (304 K), the frequency correlation in the red part of the $\nu = 0$ to 1 spectrum is destroyed within 50 fs, whereas it persists for somewhat longer times in the blue part.

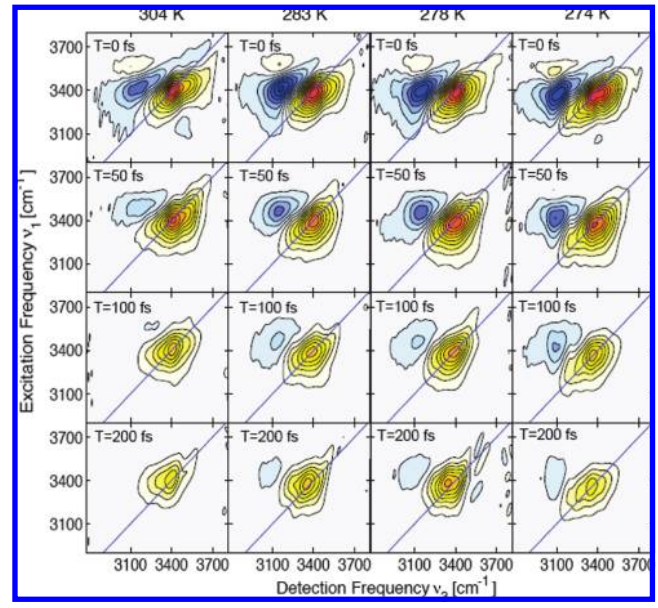

FIGURE 5. Absorptive 2D spectra of the OH stretching mode of liquid H_2O for different population times T and sample temperatures (taken from ref 39). Spectra for temperatures of 304, 283, 278, and 274 K are arranged in columns. The plots for each set of temperatures are normalized to the peak amplitude of the $\nu = 0$ to 1 transition at $T = 0$ fs. Contour lines correspond to 10% changes in amplitude.

After about 200 fs, the 2D spectra show that the frequencies are randomized. For lower temperatures, spectral diffusion slows with the major decrease of frequency correlation, however still occurring within the first 200 fs. Because of the short ($\nu = 1$) lifetime of the OH stretching mode of 200 fs, 2D spectra at longer population times are strongly influenced by the redistribution of vibrational energy and, thus, give limited insight into frequency correlations.

The sub-50-fs spectral diffusion originates mainly from the high-frequency components of the fluctuating Coulomb forces the polar water molecules in the liquid exert on the OH stretch oscillator probed. Thus, the relevant molecular motions are in this time range. The hydrogen-bond mode changing the O···O distance between neighboring water molecules has a vibrational period of 170 fs, too long to play a dominant role here. Instead, high-frequency hindered rotations of water molecules, so-called librations, change the relative orientation of neighboring water molecules and generate high-frequency components of the fluctuating force. Liquid water displays a broad librational spectrum up to frequencies of 1700 cm^{-1},[40] covering the relevant ultrafast time range. From a structural point of view, the molecular configuration around an excited OH stretching oscillator changes within 50 fs significantly enough to destroy a major part of correlation between the ini-

tial and the final configuration. This behavior is equivalent to an ultrafast loss of structural memory in the liquid.

In neat H_2O, the transfer of OH stretching excitations between neighboring water molecules with slightly different transition frequencies $\nu(0-1)$ occurs on a 50−100 fs time scale.[16,39] At low temperatures, energy transfer is faster than the loss of frequency correlation, resulting in a delocalization of the initially coherent OH stretching excitation over several water molecules. Energy transfer is mediated by the coupling of the OH stretch transition dipoles of the molecules involved. In the incoherent limit, for example, at 304 K, energy transfer between oscillators with different $\nu(0-1)$ results in spectral diffusion and dephasing. Recent theoretical work has shown that energy transfer on a 50−100 fs time scale can be accounted for with a moderate intermolecular dipole coupling of ∼20 cm^{-1}.[41,42]

A comment should be made on vibrational relaxation and energy dissipation in liquid H_2O. The $\nu = 1$ state of the OH stretching mode is in Fermi resonance with the $\nu = 2$ state of the OH bending mode. The OH stretching mode with a $\nu = 1$ lifetime of 200 fs decays via the $\nu = 2$ and $\nu = 1$ states of the OH bending mode in a stepwise process.[43] The $\nu = 1$ lifetime of the OH bending mode has a value of 170 fs. The vibrational energy released in this process is transferred to intermolecular modes such as librations of the hydrogen-bond network. In addition to energy relaxation of excited water molecules, the formation of a hot ground state requires the delocalization of excess energy within the molecular network, a process completed within 5 ps after excitation.[43]

5. Outlook: Vibrational Dynamics of Hydrated DNA

Hydrated DNA combines quasi-static and fluctuating hydrogen-bonded structures. The pairing of nucleic bases in the double helix involves different quasi-static N−H···N and N−H···O hydrogen bonds. Hydration of DNA involves interactions of water molecules with specific binding sites at the bases and with the ionic phosphate groups of the DNA backbone. Beyond this so-called first solvation shell, there are additional water molecules in the surrounding, forming a fluctuating molecular network. The microscopic structural dynamics occur to a large extent in the ultrafast time domain, and femtosecond vibrational spectroscopy can provide basic new insight into the relevant interactions.[44]

Vibrational spectra of hydrated DNA are highly congested and an assignment of the overlapping or closely spaced vibrational bands is essential for monitoring and understanding

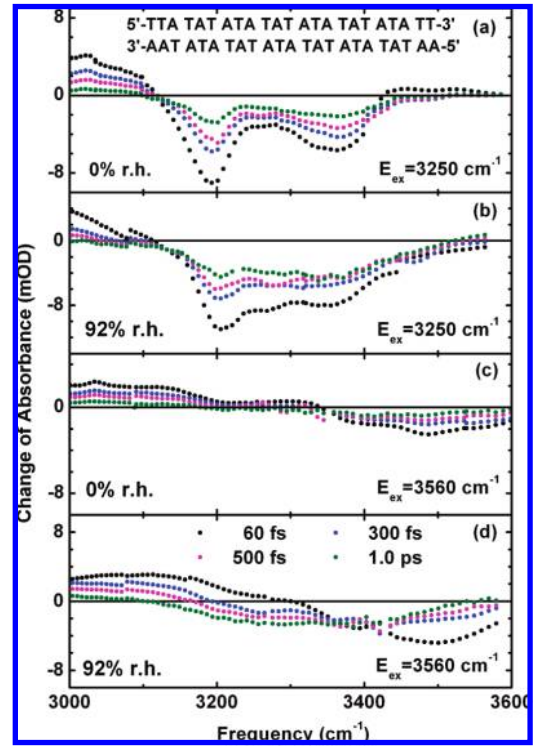

FIGURE 6. Transient vibrational spectra of DNA oligomers (inset of panel a) after excitation at (a, b) $E_{ex} = 3250$ cm^{-1} or (c,d) $E_{ex} = 3560$ cm^{-1} for different pump−probe delays (symbols, inset of panel d). Data are shown for hydration levels of 0% relative humidity (RH) and 92% RH. The spectra display NH stretching bands of the adenine−thymine base pairs with maxima at 3250 and 3335 cm^{-1} and the broad OH stretching absorption of water.

microscopic dynamics. In Figure 1c, the infrared absorption of double-stranded DNA oligomers containing 23 alternating adenine−thymine (A−T) base pairs in a helix geometry is shown for two hydration levels. The absorption in the frequency range between 3000 and 3700 cm^{-1} is due to the different N−H stretching bands of A and T and the O−H stretching absorption of water. A separation of such bands has not been possible in such linear spectra but has been accomplished by recent femtosecond two-color pump−probe studies.[45,46] Pump−probe spectra for two different excitation conditions and different delay times are presented in Figure 6. In such experiments, an isotropic film of DNA oligomers with sodium counterions replaced by surfactant molecules was studied at well-defined levels of hydration. A value of 0% relative humidity (RH) corresponds to two water molecules per base pair, whereas the oligomers are fully hydrated with more than 20 water molecules per base pair at 92% RH. The pump−probe spectra for 0% RH reveal three distinct bands with maxima at 3200, 3350, and 3500 cm^{-1} that undergo negligible spectral diffusion on a time scale of up to 5 ps. The band at 3200 cm^{-1} is due to a superposition of the NH

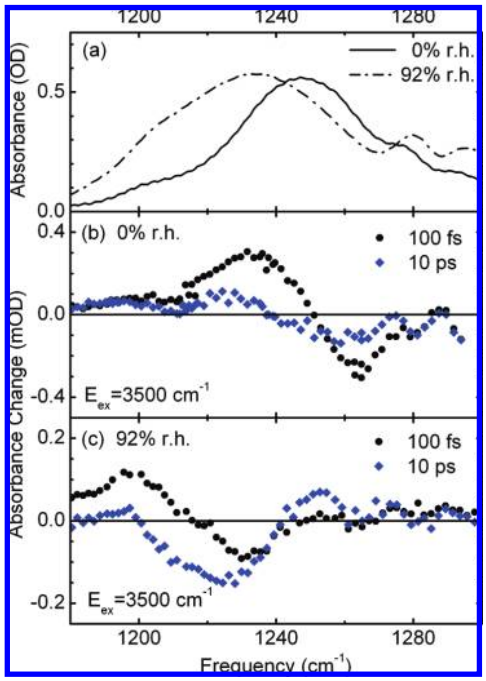

FIGURE 7. (a) Absorption band of the asymmetric phosphate $(PO_2)^-$ stretching vibration of DNA oligomers for 0% and 92% RH. (b,c) Transient spectra of the phosphate stretching mode after excitation of the OH stretching vibration of water molecules interacting with DNA. Data for 0% and 92% RH are shown for time delays of 100 fs (circles) and 10 ps (diamonds) after excitation at E_{ex} = 3500 cm^{-1}.

stretching mode of thymine and the symmetric NH_2 stretching mode of adenine. This assignment is supported by measurements of the pump−probe anisotropy as has been discussed in ref 46. The band at 3350 cm^{-1} is caused by the asymmetric NH_2 stretching mode of adenine, and the band at 3500 cm^{-1} is due to the OH stretching mode of water. At 0% RH, the two water molecules per base pair are located at the phosphate groups of the DNA backbone with negligible excitation transfer or rotational reorientation.

At 92% RH, the spectral positions of the NH stretching bands remain essentially unchanged and are superimposed by the broad OH stretching absorption of water. Detailed inspection of the transient OH stretching bands shows that in addition to the water molecules fixed at the phosphates, there is a second species with properties closer to bulk water (see section 4). This species displays subpicosecond spectral diffusion, a $\nu = 1$ lifetime closer to bulk water, and a hot vibrational ground state formed by the decay of the OH stretching excitation.[46]

The asymmetric $(PO_2)^-$ stretching vibration of the phosphate groups located in the DNA backbone is highly sensitive to interactions with water molecules (Figure 7a[47]). Results of the first femtosecond study of phosphate dynamics are presented in Figure 7b,c. The change of phosphate absorption after excitation of the OH stretching vibration of water is plotted as a function of probe frequency for 0% and 92% RH and delay times of 100 fs and 10 ps. The spectra at 100 fs display a red-shift of the phosphate stretching absorption due to vibrational coupling to the OH stretching oscillators. After 10 ps, the OH stretching excitations have decayed, and the spectra reflect the phosphate absorption in a heated vibrational ground state. The different behavior at the two hydration levels point to different couplings and hydrogen-bond dynamics as will be discussed elsewhere.

In conclusion, the pump−probe results presented are essential for understanding the vibrational spectra and dynamics of hydrated DNA. They pave the way for more detailed studies of the 2D NH and OH stretching spectra and of the interaction of water molecules with the ionic phosphate groups.

I would like to thank Erik T. J. Nibbering, Nils Huse, Satoshi Ashihara, Lukas Szyc, Ming Yang, Jason Dwyer, Jens Dreyer, Karsten Heyne, Max-Born-Institut, and Michael Cowan, Barry Bruner, Alex Paarmann, Darren Kraemer, and Dwayne Miller, University of Toronto, for their important contributions to the work described here. Financial support by the Deutsche Forschungsgemeinschaft and the Fonds der Chemischen Industrie is gratefully acknowledged.

BIOGRAPHICAL INFORMATION

Thomas Elsaesser received a Diploma and a Dr. rer. nat. degree in physics from the Technical University of Munich (TU Munich) in 1982 and 1986. He worked as a research associate at the Physics Department of the TU Munich from 1986 until 1993. After spending a postdoctoral period at AT&T Bell Laboratories, Holmdel, NJ, he finished his habilitation at the TU Munich in 1991. Since 1993, Thomas Elsaesser has been a director of the Max-Born-Institute and holds a joint appointment with the Institute of Physics of Humboldt University. Ultrafast phenomena in condensed matter represent the main area of his research. Major topics are transient structures of (bio)molecules and solids as well as the investigation of basic microscopic interactions in solids and liquids for which a broad range of optical and X-ray techniques are applied. Such work has resulted in more than 330 publications in refereed journals and books and six patents. Thomas Elsaesser received the Rudolf Kaiser Prize in 1991 and the Otto Klung Award in Physics in 1995. In 2004, he was with the Ecole Normale Superieure in Paris as a Professeur invité. Presently, he serves as a Director at large on the Board of Directors of the Optical Society of America.

REFERENCES

1 Pimentel, G. L.; McClellan, A. L. *The Hydrogen Bond*; W.H. Freeman: San Francisco, CA, 1960.

2 Schuster, P., Zundel, G., Sandorfy, C., Eds. *The Hydrogen Bond: Recent developments in theory and experiments*; North Holland: Amsterdam, 1976.

3 Fayer, M. D., Ed. *Ultrafast infrared and Raman spectroscopy*; Marcel Dekker: New York, 2001.

4 Nibbering, E. T. J.; Elsaesser, T. Ultrafast vibrational dynamics of hydrogen bonds in the condensed phase. *Chem. Rev.* **2004**, *104*, 1887–1914.

5 Hamm, P.; Lim, M.; Hochstrasser, R. M. Structure of the amide I band of peptides measured by femtosecond nonlinear-infrared spectroscopy. *J. Phys. Chem. B* **1998**, *102*, 6123–6138.

6 Asplund, M. C.; Zanni, M. T.; Hochstrasser, R. M. Two dimensional infrared spectroscopy of peptides by phase-controlled femtosecond vibrational photon echoes. *Proc. Natl. Acad. Sci. U.S.A.* **2000**, *97*, 8219–8224.

7 Mukamel, S. Multidimensional femtosecond correlation spectroscopies of electronic and vibrational excitations. *Annu. Rev. Phys. Chem.* **2000**, *51*, 691–729.

8 Okumura, K.; Tokmakoff, A.; Tanimura, Y. Two-dimensional line-shape analysis of photon-echo signal. *Chem. Phys. Lett.* **1999**, *314*, 488–495.

9 Jonas, D. M. Two-dimensional femtosecond spectroscopy. *Annu. Rev. Phys. Chem.* **2003**, *54*, 425–463.

10 Kaindl, R. A.; Wurm, M.; Reimann, K.; Hamm, P.; Weiner, A. M.; Woerner, M. Generation, shaping, and characterization of intense femtosecond pulses tunable from 3 to 20 μm. *J. Opt. Soc. Am. B* **2000**, *17*, 2086–2094.

11 Reimann, K.; Smith, R. P.; Weiner, A. M.; Elsaesser, T.; Woerner, M. Direct field-resolved detection of terahertz transients with amplitudes of megavolts per centimeter. *Opt. Lett.* **2003**, *28*, 471–473.

12 Heyne, K.; Huse, N.; Nibbering, E. T. J.; Elsaesser, T. Ultrafast coherent nuclear motions of hydrogen bonded carboxylic acid dimers. *Chem. Phys. Lett.* **2003**, *369*, 591–596.

13 Cervetto, V.; Helbing, J.; Bredenbeck, J.; Hamm, P. Double-resonance versus pulsed Fourier transform two-dimensional infrared spectroscopy: An experimental and theoretical comparison. *J. Chem. Phys.* **2004**, *121*, 5935–5942.

14 Graener, H.; Seifert, G.; Laubereau, A. New spectroscopy of water using tunable picosecond pulses in the infrared. *Phys. Rev. Lett.* **1991**, *66*, 2092–2095.

15 Gale, G. M.; Gallot, G.; Hache, F.; Lascoux, N.; Bratos, S.; Leicknam, J. C. Femtosecond dynamics of hydrogen bonds in liquid water: A real time study. *Phys. Rev. Lett.* **1999**, *82*, 1068–1071.

16 Cowan, M. L.; Bruner, B. D.; Huse, N.; Dwyer, J. R.; Chugh, B.; Nibbering, E. T. J.; Elsaesser, T.; Miller, R. J. D. Ultrafast memory loss and energy redistribution in the hydrogen bond network of liquid H_2O. *Nature* **2005**, *434*, 199–202.

17 Maréchal, Y.; Witkowski, A. Infrared spectra of H-bonded systems. *J. Chem. Phys.* **1968**, *48*, 3697–3705.

18 Henri-Rousseau, O.; Blaise, P.; Chamma, D. Infrared line shapes of weak hydrogen bonds: Recent quantum developments. *Adv. Chem. Phys.* **2002**, *121*, 241–309.

19 Emmeluth, C.; Suhm, M. A.; Luckhaus, D. A monomers-in-dimers model for carboxylic acid dimers. *J. Chem. Phys.* **2003**, *118*, 2242–2255.

20 Rösch, N.; Ratner, M. Model for the effects of a condensed phase on the infrared spectra of hydrogen-bonded systems. *J. Chem. Phys.* **1974**, *61*, 3344–3351.

21 Oxtoby, D. W. Dephasing of molecular vibrations in liquids. *Adv. Chem. Phys.* **1979**, *40*, 1–48.

22 Heyne, K.; Huse, N.; Dreyer, J.; Nibbering, E. T. J.; Elsaesser, T.; Mukamel, S. Coherent low-frequency motions of hydrogen bonded acetic acid dimers in the liquid phase. *J. Chem. Phys.* **2004**, *121*, 902–913.

23 Huse, N.; Heyne, K.; Dreyer, J.; Nibbering, E. T. J.; Elsaesser, T. Vibrational multilevel quantum coherence due to anharmonic couplings in intermolecular hydrogen bonds. *Phys. Rev. Lett.* **2003**, *91*, 197401.

24 Huse, N.; Bruner, B. D.; Cowan, M. L.; Dreyer, J.; Nibbering, E. T. J.; Miller, R. J. D.; Elsaesser, T. Anharmonic couplings underlying the ultrafast vibrational dynamics of hydrogen bonds in liquids. *Phys. Rev. Lett.* **2005**, *95*, 147402.

25 Dreyer, J. Hydrogen-bonded acetic acid dimers: Anharmonic coupling and linear infrared spectra studied with density functional theory. *J. Chem. Phys.* **2005**, *122*, 184306.

26 Dreyer, J. Density functional theory simulations of two-dimensional infrared spectra for hydrogen-bonded acetic acid dimers. *Int. J. Quantum Chem.* **2005**, *104*, 782–793.

27 Elsaesser, T.; Huse, N.; Dreyer, J.; Dwyer, J. R.; Heyne, K.; Nibbering, E. T. J. Ultrafast vibrational dynamics and anharmonic couplings of hydrogen-bonded dimers in solution. *Chem. Phys.* **2007**, *341*, 175–188.

28 Rey, R.; Moller, K. B.; Hynes, J. T. Hydrogen bond dynamics in water and ultrafast infrared spectroscopy. *J. Phys. Chem. A* **2002**, *106*, 11993–11996.

29 Woutersen, S.; Bakker, H. J. Resonant intermolecular transfer of vibrational energy in liquid water. *Nature* **1999**, *402*, 507–509.

30 Woutersen, S.; Bakker, H. J. Hydrogen bond in liquid water as a Brownian oscillator. *Phys. Rev. Lett.* **1999**, *83*, 2077–2080.

31 Stenger, J.; Madsen, D.; Hamm, P.; Nibbering, E. T. J.; Elsaesser, T. Ultrafast vibrational dephasing of liquid water. *Phys. Rev. Lett.* **2001**, *87*, 027401.

32 Stenger, J.; Madsen, D.; Hamm, P.; Nibbering, E. T. J.; Elsaesser, T. A photon echo peak shift study of liquid water. *J. Phys. Chem. A* **2002**, *106*, 2341–2350.

33 Yeremenko, S.; Pshenichnikov, M. S.; Wiersma, D. A. Hydrogen-bond dynamics in water explored by heterodyne-detected photon echo. *Chem. Phys. Lett.* **2003**, *369*, 107–113.

34 Fecko, C. J.; Eaves, J. D.; Loparo, J. J.; Tokmakoff, A.; Geissler, P. L. Ultrafast hydrogen-bond dynamics in the infrared spectroscopy of water. *Science* **2003**, *301*, 1698–1702.

35 Ashbury, J. B.; Steinel, T.; Stromberg, C.; Corcelli, S. A.; Lawrence, C. P.; Skinner, J. L.; Fayer, M. D. Water dynamics: Vibrational echo correlation spectroscopy and comparison to molecular dynamics simulations. *J. Phys. Chem. A* **2004**, *108*, 1107–1119.

36 Piryatinski, A.; Lawrence, C. P.; Skinner, J. L. Vibrational spectroscopy of HOD in liquid D_2O. V. Infrared three-pulse photon echoes. *J. Chem. Phys.* **2003**, *118*, 9672–9679.

37 Moller, K. B.; Rey, R.; Hynes, J. T. Hydrogen bond dynamics in water and ultrafast infrared spectroscopy: a theoretical study. *J. Phys. Chem. A* **2004**, *108*, 1275–1289.

38 Eaves, J. D.; Loparo, J. J.; Fecko, C. J.; Roberts, S. T.; Tokmakoff, A.; Geissler, P. L. Hydrogen bonds in liquid water are broken only fleetingly. *Proc. Natl. Acad. Sci. U.S.A.* **2005**, *102*, 13019–13022.

39 Kraemer, D.; Cowan, M. L.; Paarmann, A.; Huse, N.; Nibbering, E. T. J.; Elsaesser, T.; Miller, R. J. D. Temperature dependence of the two-dimensional infrared spectrum of liquid H_2O. *Proc. Natl. Acad. Sci. U.S.A.* **2008**, *105*, 437–442.

40 Walrafen, G. E.; Blatz, L. A. Weak Raman bands from water. *J. Chem. Phys.* **1973**, *59*, 2646–2650.

41 Paarmann, A.; Hayashi, S.; Mukamel, S.; Miller, R. J. D. Probing intermolecular couplings in liquid water with two-dimensional infrared photon echo spectroscopy. *J. Chem. Phys.* **2008**, *128*, 191103.

42 Auer, B. M.; Skinner, J. L. IR and Raman spectra of liquid water: Theory and interpretation. *J. Chem. Phys.* **2008**, *128*, 224511.

43 Ashihara, S.; Huse, N.; Espagne, A.; Nibbering, E. T. J.; Elsaesser, T. Ultrafast structural dynamics of water induced by dissipation of vibrational energy. *J. Phys. Chem A* **2007**, *111*, 743–746.

44 Krummel, A. T.; Zanni, M. T. DNA vibrational coupling revealed with two-arared spectroscopy: insight into why vibrational spectroscopy is sensitive to DNA structure. *J. Phys. Chem. B* **2006**, *110*, 13991–14000.

45 Dwyer, J. R.; Szyc, L.; Nibbering, E. T. J.; Elsaesser, T. Ultrafast vibrational dynamics of adenine-thymine base pairs in DNA oligomers. *J. Phys. Chem. B* **2008**, *112*, 11194–11197.

46 Szyc, L.; Dwyer, J. R.; Nibbering, E. T. J.; Elsaesser, T. Ultrafast dynamics of NH and OH stretching excitations in hydrated DNA oligomers. *Chem. Phys.* **2009**, *357*, 36–44.

47 Falk, M.; Hartman, K. A.; Lord, R. C. Hydration of DNA. II. An infrared study. *J. Am. Chem. Soc.* **1963**, *85*, 387–391.